Zeitschrift: Eclogae Geologicae Helvetiae
Herausgeber: Schweizerische Geologische Gesellschaft
Band: 83 (1990)
Heft: 3: The Hans Laubscher volume

Artikel: Unique determination of normal fault shape from hanging-wall bed geometry in detached half grabens

Autor: Groshong, Richard H.

DOI: https://doi.org/10.5169/seals-166596

Eclogae geol. Helv. 83/3: 455–471 (1990)

0012-9402/90/030455–17 $ 1.50 + 0.20/0
Birkhäuser Verlag, Basel

Unique determination of normal fault shape from hanging-wall bed geometry in detached half grabens

By Richard H. Groshong, Jr.[1])

ABSTRACT

The oblique-simple-shear cross-section drawing technique that relates the shape of a bed in the hanging-wall rollover above a detached normal fault to the shape of the fault does not provide a unique solution unless the dip of the simple shear plane is known. The magnitude of the layer-parallel strain proves to be a constraint that allows the fault shape to be uniquely determined by this method. The layer-parallel strain in the rollover depends upon the dip of the shear plane and the amount of simple shear, the latter being a function of the dip in the rollover. If the dip and the layer-parallel strain in a key bed can be measured, then the dip of the shear plane can be calculated. The shear-plane dip, smoothed hanging-wall bed shape, and offset on the master fault are used to predict the master fault shape by the method of oblique simple shear. The computed dip of the shear plane is fairly sensitive to the strain in the rollover; consequently the strain provides a tight constraint on the fault geometry. The inversion technique works well with experimental models and provides a geologically reasonable master fault shape when applied to a seismic cross section of the Malawi rift.

ZUSAMMENFASSUNG

Die Querprofil-Konstruktionsmethode der schiefen einfachen Scherung, welche die Geometrie einer Schicht im Rollover der Hangendscholle über einer Abschiebung mit der Geometrie der Abscherfläche in Beziehung setzt, erbringt ausser in den Fällen, wo das Einfallen der Scherfläche bekannt ist, keine eindeutige Lösung. Die schichtparallele Deformation erweist sich nun als eine kritische Grösse, mit welcher sich die Geometrie der Abschiebungsfläche mit dieser Methode dennoch eindeutig bestimmen lässt. Die schichtparallele Deformation im Rollover hängt von der Neigung der Scherfläche und dem Betrag der einfachen Scherung ab, wobei letzterer eine Funktion des Einfallens des Rollovers ist. Können Einfallen und schichtparallele Deformation eines Referenzhorizontes bestimmt werden, so lässt sich daraus das Einfallen der Scherfläche berechnen. Das Einfallen der Scherfläche, die ausgeglättete Geometrie der Schichten der Hangendscholle, sowie der Versatz auf der Hauptbruchfläche werden verwendet, um die Geometrie der Bruchfläche mit der Methode der schiefen einfachen Scherung zu bestimmen. Da der errechnete Einfallbetrag der Scherfläche recht empfindlich auf Änderungen des Deformationsbetrages im Rollover reagiert, lässt sich mit Hilfe der Deformation die Geometrie des Bruches eng eingrenzen. Diese Inversionstechnik führt zu guten Resultaten für experimentelle Modelle und ergibt eine geologisch vernünftige Geometrie der Hauptabschiebungsfläche bei der Interpretation eines seismischen Profils durch das Malawi Rift.

Introduction

A long-standing goal in structural analysis is the correct interpretation of the deep structure from shallow and/or incomplete data. The currently most successful approach for the direct inversion of shallow data into a complete, internally consistent cross section is the method of balancing cross sections (Chamberlin 1910; Bucher

[1]) Department of Geology. The University of Alabama, Tuscaloosa, AL 35487–0338, USA.

1933; Laubscher 1962, 1965; Bally et al. 1966; Dahlstrom 1969; Gibbs 1983; Woodward et al. 1989), a technique that has evolved from a test of cross section geometry into a methodology for drawing complete cross sections from partial data (Verrall 1981; Suppe 1983; Geiser et al. 1988; Rowan & Kligfield 1989). There is no unique balancing method, however. Different methods are required for different structural styles and a variety of alternatives are seemingly possible for even a single style. Most extensional structural styles fall into one of four major groups (Fig. 1): full grabens, independent half grabens, domino half grabens, and rotational glide-block graben systems. Cross sections of one style, independent half grabens developed above listric or ramp-and-flat faults, can in favorable circumstances be uniquely inverted to find the fault shape if the strain in the hanging-wall is known. All four styles are briefly described in order to better characterize the style of interest here.

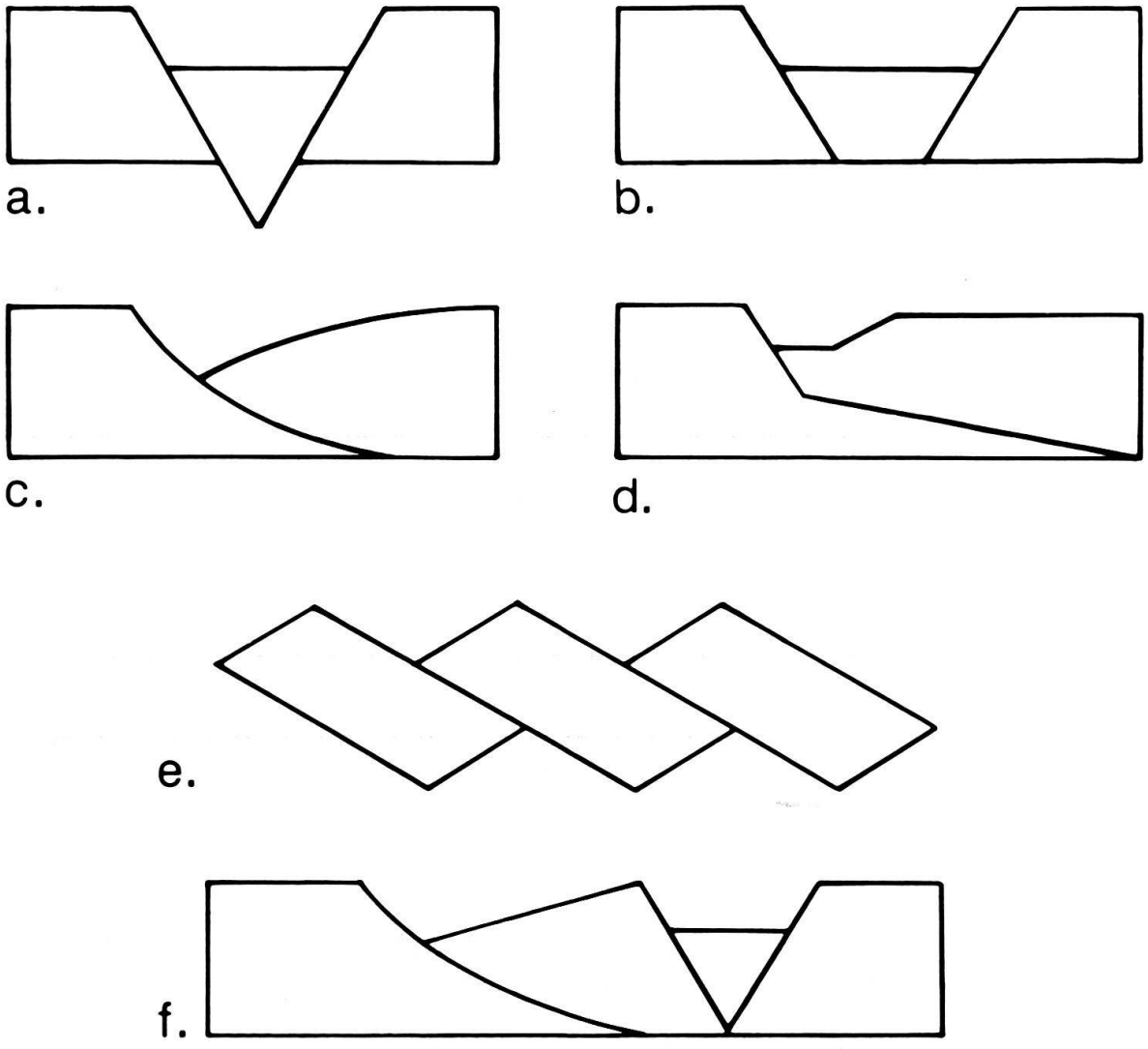

Fig. 1. Extensional structural styles. (a) Undeformed full graben. (b) Deformed full graben above detachment. (c) Independent half graben above listric master fault. (d) Independent half graben above ramp-and-flat master fault. (e) Domino half grabens. (f) Rotational glide-block system.

A full graben (Rosendahl 1987) is bounded on both sides by normal faults having nearly equal amounts of displacement. An undeformed full graben (Fig. 1a) can develop where the region below the faulted layer moves to make space for the graben. This style is produced experimentally if the graben can drop into an open space (Cloos 1968). Internally deformed full grabens (Fig. 1b) occur above a detachment. This style has been produced experimentally by non-uniform extension above a stretched detachment (Stewart 1971) and by earthquake-induced slope failure (Hansen 1965). Profiles across the Rhine Graben between Speyer and Karlsruhe show it to be a relatively symmetrical, internally deformed full graben (Doebl & Teichmüller 1979) as are the detached grabens of the Dinkelberg-Tabular Jura (Laubscher 1982). Large-scale extension accommodated by small displacements on many conjugate faults may result in small but relatively undeformed full grabens (McClay & Ellis 1987a, 1987b).

There are several types of half grabens. A half graben is bounded on one side by a master fault and on the other by a limb that dips toward the master fault. One type of half graben develops above a listric fault which may show either smooth curvature (Fig. 1c) or a ramp-and-flat style (Fig. 1d). This style is here termed an independent half graben because the graben is not necessarily linked to any other graben and to distinguish the style from domino half grabens which must be kinematically linked to adjacent domino half grabens. In an independent half graben, the limb dip toward the master fault has been termed reverse drag by Hamblin (1965) and antithetic dip by

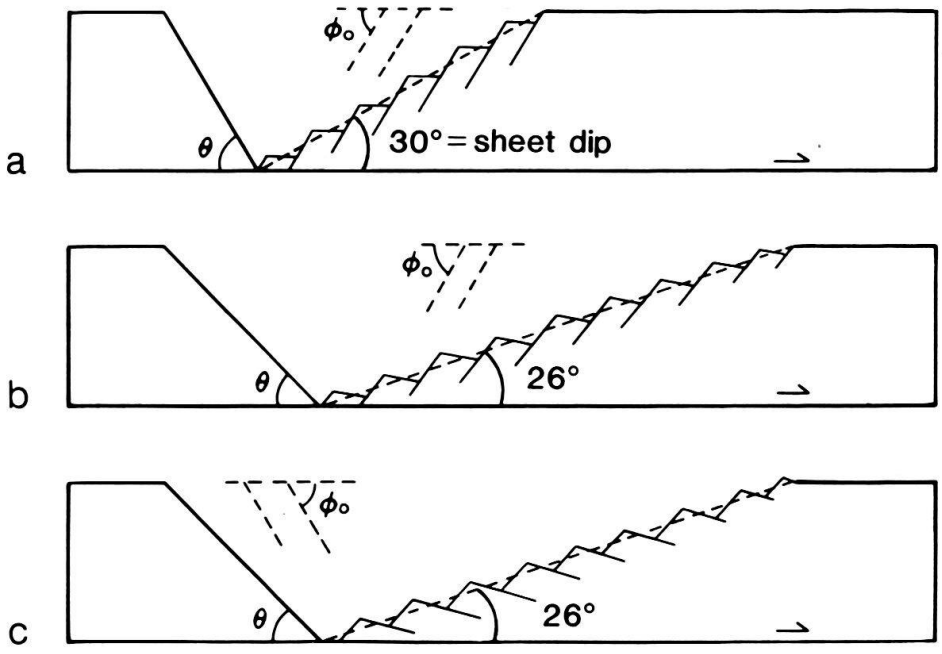

Fig. 2. Ramp-and-flat independent half grabens with domino-block extension in the rollover. Relationship between dip of the master fault, Θ, and dip and amount of extension in the rollover from Groshong (1989). Domino-block geometry from equation 9; Φ_0 = cutoff angle of domino-bounding fault. (a) Domino-block faults begin exactly antithetic to 60° dipping master fault: bedding in limb remains horizontal. (b) Domino-block faults (60° dip) begin antithetic to but steeper than 45° dipping master fault: bedding in limb dips away from master fault. (c) Domino-block faults (60° dip) begin synthetic to but steeper than 45° dipping master fault: bedding in limb dips toward master fault.

GROSHONG (1989), and it is commonly called rollover in Gulf of Mexico thin-skinned structures. The latter term will be used here. The hanging wall in the rollover is characteristically faulted and the local dip of bedding in a fault block may differ from the sheet dip (MCCLAY 1987). The sheet dip of a faulted bed is the dip of a surface drawn through equivalent points of the bed in adjacent fault blocks (i.e., through the centers of the blocks, Fig. 2a). Structures having geometries ranging from 1c to 1d are produced experimentally where extension is localized above a planar lower detachment (CLOOS 1968; MCCLAY & ELLIS 1987a).

Domino half grabens (Fig. 1e) are the result of rigid body rotation or near-rigid body rotation of fault-bounded blocks. Both bedding and the faults rotate as extension increases. Because both hanging wall and footwall rotate, domino half grabens are not independent of one another and occur as multiple half grabens of the same age. Domino blocks are consistently produced experimentally above an extending detachment when there is a uniform sense of shear on the detachment. The shear sense results either from the slope of the detachment (MCCLAY & ELLIS 1987b; VENDEVILLE et al. 1987) or from the slope of the free surface of the model (MANDL 1987). The fault dip is such that the hanging-wall displacement is in the direction of hanging-wall shear at the detachment (MANDL 1987).

What is here called a rotational glide-block graben system (Fig. 1f) consists of a rotated block (the glide-block in the terminology of ARMSTRONG 1972) that rigidly rotates between a listric master fault and an adjacent kinematically necessary (MCCLAY & ELLIS 1987b; ELLIS & MCCLAY 1988) full graben that separates the rotated block from the undeformed but translated portion of the hanging-wall. This style has been produced experimentally by displacing the hanging wall along a precut listric fault (MCCLAY & ELLIS 1987a, 1987b; ELLIS & MCCLAY 1988) and is a common mode of slope failure at the up-dip end of a slump (HANSEN 1965).

Different styles in Figure 1 may be transitional into one another or may occur in combination. Small rotational glide blocks may occur against the master fault of an independent half graben (WERNICKE & BURCHFIEL 1982) and are called riders by GIBBS (1984). The limb of an independent half graben is commonly internally deformed by a domino-style mechanism (Fig. 2). Internal deformation of the blocks themselves, such as interpreted by GIBSON et al. (1989), might occur within the context of any of the four styles. Master low-angle normal faults (WERNICKE & BURCHFIEL 1982) may be the lower portions of listric or ramp-flat independent half-graben systems or may represent the detachment zone at the base of a region of domino extension (LE PICHON & SIBUET 1981; MILLER et al. 1983).

This paper is concerned with the independent half-graben style of extension, in which the master fault may be either smoothly curved or ramp-and-flat in shape. The style is recognized as being very important in thin-skinned structures (ASHFORD 1972; BALLY & SNELSON 1980; VERRALL 1981) and in basement-involved structures (BALLY & SNELSON 1980; GIBBS 1983, 1984; EYIDOGAN & JACKSON 1985; BEACH 1986; WHITE et al. 1986; ROSENDAHL 1987; CRESPI 1988; SCOTT & ROSENDAHL 1989).

VERRALL (1981) was first to publish a method for inverting the extensional rollover geometry in an independent half graben to obtain the shape of the master fault. His method is based on the assumption of constant heave and models the hanging-wall geometry as being the result of vertical simple shear; vertical slip between adjacent in-

finitesimally thin segments is in the amount necessary to maintain contact between the base of the hanging wall and the fault. The fault geometry may be constructed by hand and, given the fault geometry, the shape of any bed in the hanging-wall may be found (VERRALL 1981). This model has been generalized by WHITE et al. (1986) and WHITE 1987) to include oblique simple shear; vertical simple shear is a special case. A version for ramp-and-flat master faults in which the oblique simple shear is antithetic to the ramp has been developed by GROSHONG (1989). Other inversion techniques have been proposed. A method based on the assumption of constant displacement along slip lines parallel to the fault (WILLIAMS & VANN 1987) in general requires shear in the hanging wall outside the rollover (WILLIAMS & VANN 1987; WHEELER 1987) and does not necessarily preserve area (WHEELER 1987). Constant bed length techniques have also been presented and are based on the concept of layer-parallel slip (SUPPE 1983; DAVISON 1986; ROWAN & KLIGFIELD 1989). Numerous authors have noted the lack of uniqueness of the inversion methods (WHITE et al. 1986; WILLIAMS & VANN 1987; CRESPI 1988; GROSHONG 1989; ROWAN & KLIGFIELD 1989). Current empirical experience, based on fitting rollover geometries to known fault planes, suggests that vertical simple shear is approximately correct for thin-skinned structures (VERRALL 1981; ROWAN & KLIGFIELD 1989) and vertical to antithetic shear planes are most suitable for basement-involved structures (WHITE et al. 1986; CRESPI 1988; GROSHONG 1989; ROWAN & KLIGFIELD 1989; ROWAN, personal communication).

Beds within the rollover of an independent half graben are typically stretched as indicated by offsets along normal faults within the rollover. Extension within the rollover is characteristic of experimental models (CLOOS 1968; MCCLAY & ELLIS 1987a, 1987b). WERNICKE & BURCHFIEL (1982) and ROSENDAHL (1987) clearly showed domino-like extension within the rollover in field examples. In many examples, deformation in the rollover by the formation of domino blocks produces styles like those in Figure 2. Although these examples are schematic, they show quantitatively correct amounts of strain based on the half-graben model of GROSHONG (1989) and the relationships that will be developed below. Examples and models resembling Figures 2a and 2b have been illustrated by MORTON & BLACK (1975), LE PICHON & SIBUET (1981) and EYIDOGAN & JACKSON (1985). ROSENDAHL (1987) documented the occurrence of styles 2b and 2c in the East African rifts.

In the following sections it will be shown that the amount of layer-parallel strain is a function of the angle of oblique simple shear and the sheet dip of bedding in the rollover. By measuring the layer-parallel strain and sheet dip it is possible to determine the angle of simple shear. If the original position of a key bed in the rollover can be reasonably inferred, then this information together with the angle of simple shear can provide a unique solution for the geometry of the master fault. The method is demonstrated on experimental models and applied to a seismic line from the Malawi Rift Valley. Assumptions are reviewed and the restrictions and limitations on the method are discussed at the end of the paper.

Layer-parallel strain caused by oblique simple shear

The relationship between the layer-parallel strain in the rollover, the dip of bedding, and the dip of the shear plane follows from equations 14 and 17 in GROSHONG

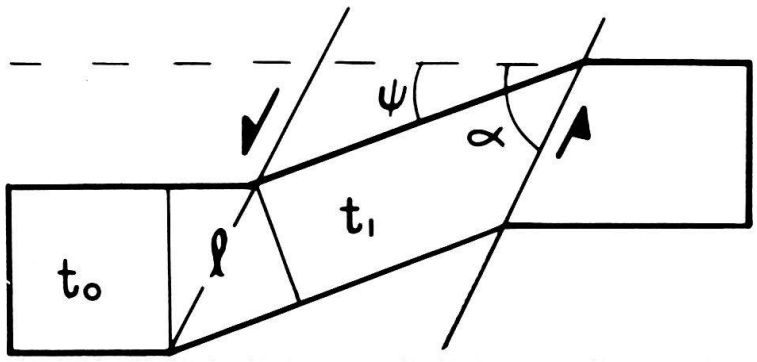

Fig. 3. Bed geometry within region of oblique simple shear.

(1989) with changes in terminology that are convenient for clarity. The dip of bedding will be called ψ (Fig. 3) because according to the model it represents the amount of shear from the horizontal. The dip of the simple-shear plane is α, the letter used by WHITE et al. (1987) and WHITE (1987) but here designates the dip rather than the hade to be more consistent with the other angle measurements. A length l parallel to the shear direction (Fig. 3) is unchanged by simple shear. At the boundary of the deformed zone, this length is equal to both $t_0/\sin\alpha$ and $t_1/\sin(\alpha-\psi)$. Equating the two gives the ratio of bed thicknesses before and after deformation.

$$t_0/t_1 = \sin\alpha/\sin(\alpha-\psi). \quad (1)$$

The strain parallel to bedding (as the change in length divided by original length) is computed from $e_\parallel = (t_0/t_1) - 1$ (equation 17, GROSHONG 1989) by replacing t_0/t_1 with the expression from equation 1:

$$e_\parallel = (\sin\alpha/\sin(\alpha-\psi)) - 1 \quad (2)$$

For vertical simple shear $\alpha = 90°$ and equation 2 simplifies to

$$e_\parallel = (1/\cos\psi) - 1 \quad (3)$$

When the strain parallel to bedding is known, equation 2 can be solved for α as:

$$\alpha = \arctan \frac{\sin\psi\,(e_\parallel + 1)}{\cos\psi\,(e_\parallel + 1) - 1}. \quad (4)$$

Equation 4 is the relationship that allows the rollover shape and strain to be inverted to find the fault profile.

The nature of the relationships embodied in equations 2–4 is illustrated in Figure 4. Bedding sheet dip, ψ, is toward the master fault. The dip of the simple shear plane is termed synthetic if it dips in the same direction as the master fault and antithetic if it dips in the opposite direction to the master fault. Shear planes having antithetic dip all produce layer-parallel extension that increases with the sheet dip of bedding. With increasing dip of bedding, shear planes having synthetic dip produce layer-parallel contraction followed by extension if the dip becomes large enough. Zero layer-parallel net strain occurs at the dip of bedding for which the shear plane bisects the bend; the bend is symmetric at that point and bed thickness is the same in the undeformed and the dipping sequence. This geometry is possible only for synthetic shear angles. For example, the strain history for a constant synthetic shear-plane dip of −80°

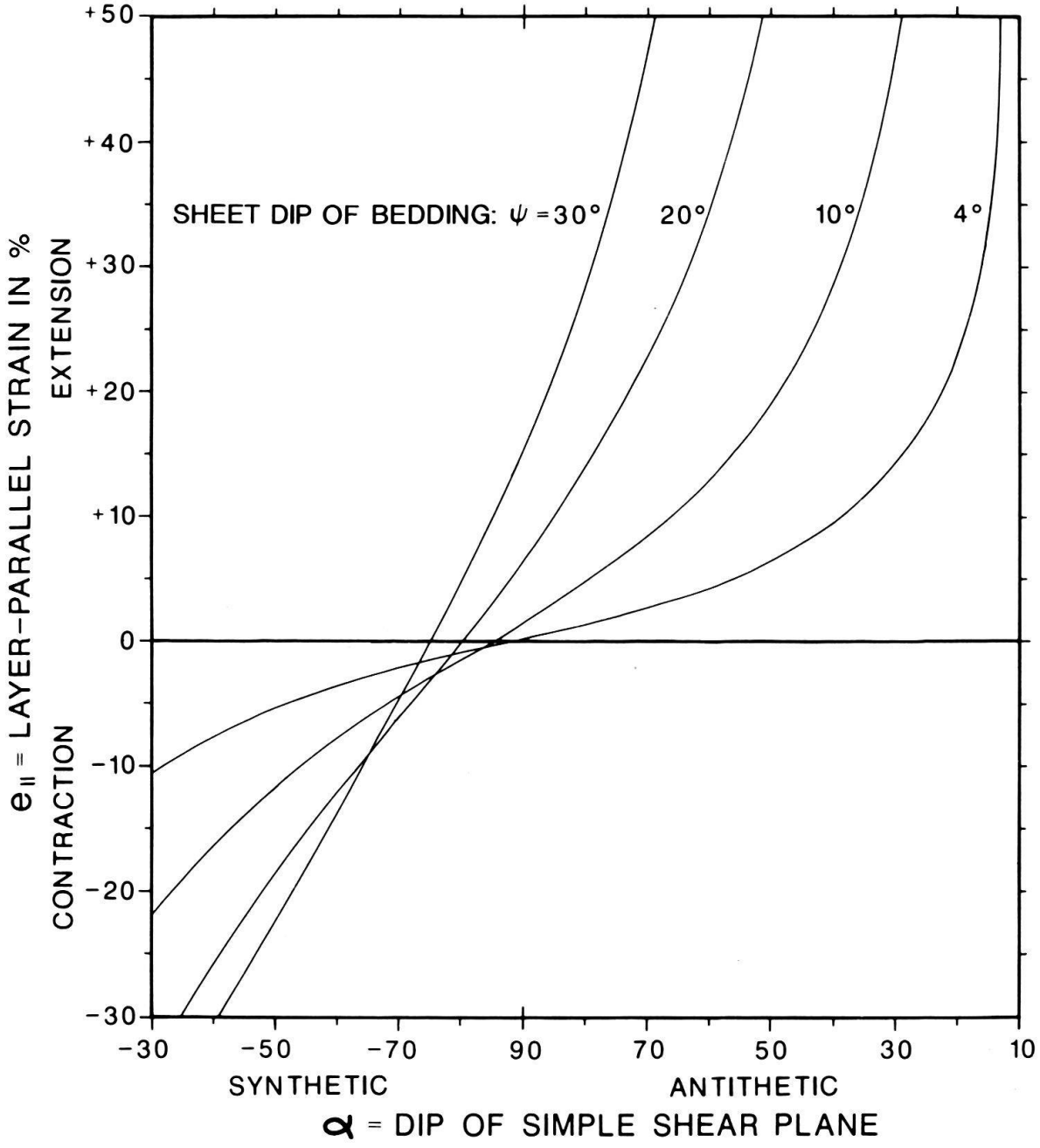

Fig. 4. Layer-parallel strain within the rollover related to the sheet dip of bedding, ψ, within the rollover and the dip of the simple shear plane, α. Constructed using equations 2 and 3.

(Fig. 4) changes from layer-parallel contraction (−1% at 4° bed dip, increasing to −1.5% at a bed dip of 10°) to layer-parallel extension, returning to zero net strain at a bed dip of 20° and then to stretching as the dip of bedding increases further (+4.5% at 30° bed dip).

The extension in the rollover is not equal to the extension of the half-graben as a whole. The half-graben extension is related to the displacement and dip on the master fault, and the angle of oblique simple shear (White et al. 1986; White 1987). The hori-

zontal displacement of the hanging-wall, D, (rewritten from WHITE et al. 1986, by changing the definition of α to be the dip of the shear plane) is:

$$D = h\,(1 + \tan \Theta_m / \tan \alpha), \quad (5)$$

where h = heave on the master fault and Θ_m = dip of the master fault segment for which the heave is measured. When the dip of the shear plane is equal and opposite to the dip of the master fault, D = 2h (WHITE 1987; GROSHONG 1989). The extension in the rollover is not added to that of equation 5 to determine the total displacement because they are separate manifestations of the same deformation.

Measurement of layer-parallel strain

At shallow crustal levels within unmetamorphosed sediments and rocks, the layer-parallel strain in the rollover appears to be accomplished almost entirely by faulting. Strain can, therefore, be found from the bed length (L_0) of a key bed in the rollover (Fig. 5), the length of the sheet dip of the same surface (L_1) and computed with the relationship

$$e_{\parallel} - (L_1 = L_0)/L_0. \quad (6)$$

In many examples the strain occurs by the rotation of a series of domino blocks for which the strain can be computed as a group, avoiding the need to measure bed length. The strain due to domino blocks that retain a horizontal sheet dip ($\psi = 0$ in Figure 5) has been calculated by a number of authors (THOMPSON 1960; MORTON & BLACK 1975; LE PICHON & SIBUET 1981; WERNICKE & BURCHFIEL 1982; KLIGFIELD et al. 1984; MANDL 1987; SCLATER & CÉLÉRIER 1988). AXEN (1988) computed the extension above a dipping detachment. Of interest here is the situation in which the sheet dip of bedding in the domino blocks is tilted as a result of the rotation caused by the formation of the rollover.

The sheet dip of bedding in the domino blocks (Fig. 5) is ψ from the horizontal. The angle between bedding in the domino blocks and the sheet dip is Θ^*. The original length of a bed segment is L_0 and its projection onto the sheet dip is L_1. The fault cutoff

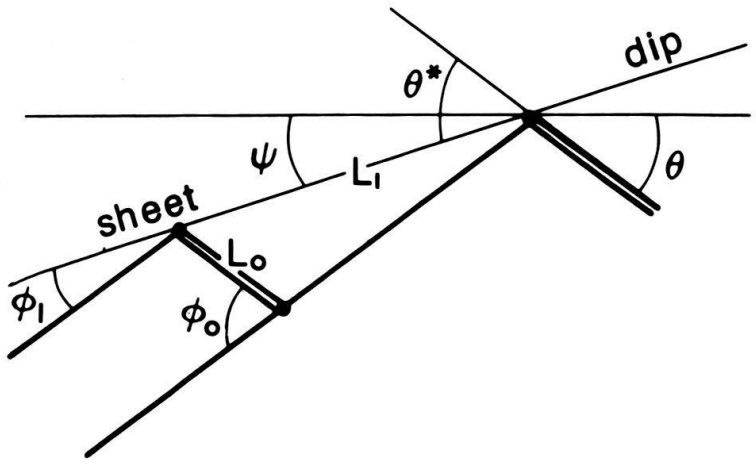

Fig. 5. Geometry of domino blocks with respect to the sheet dip of bedding. The double line is bedding. L_0 is the original length of a bed segment, L_1 is the final length of the segment in the direction of the sheet dip.

angle with bedding is Φ_0 (useage of KLIGFIELD et al. 1984) and does not change during deformation. From the law of sines, $L_1/\sin(180-\Phi_0) = L_0/\sin(\Phi_0 - \Theta^*)$ which gives

$$L_1 = L_0 \sin \Phi_0/\sin(\Phi_0 - \Theta^*). \quad (7)$$

Assuming that all the domino blocks have the same dip, equation 7 is substituted into 6 to determine the strain parallel to the sheet dip:

$$e_{\parallel} = (\sin \Phi_0/\sin(\Phi_0 - \Theta^*)) - 1. \quad (8)$$

As long as the upper corners of the blocks maintain contact with the plane of the sheet dip as in Figure 5, the strain is not sensitive to the width of the block. Many narrow blocks with small displacement accomplish the same strain as a few wide blocks. This equation ignores the ends of the series of domino blocks, leading to errors that can be ignored if there are more than 5 blocks (SCLATER & CÉLÉRIER 1988). The strain parallel to the sheet dip can be computed if the sheet dip can be determined and the necessary angle measurements of Φ_0 and Θ^* be made on a single representative fault block. If ψ is zero, then $\Theta^* = \Theta$, the dip of bedding (Fig. 5).

The geometry of domino blocks associated with a given layer-parallel strain can be computed from

$$\sin \Phi_1 = \sin \Phi_0/(e_{\parallel} + 1), \quad (9)$$

where Φ_0 is the cutoff angle of the fault and Φ_1 is the final fault dip (useage of KLIGFIELD et al. 1984), measured with respect to the sheet dip (Fig. 5). In the examples of Figure 2 the layer-parallel strain in the rollover was calculated from the antithetic shear model of GROSHONG (1989) and the domino geometry from equation 9.

Construction technique

The method for determining the fault shape uses a deformed and restored geometry of a key bed in the rollover to find the geometry of the fault by a modified version of the technique of VERRALL (1981). It is given as the series of steps required to do the reconstruction by hand. Refer to Figure 6a for the geometry.

1. Define the restored geometry. Locate a key bed in the rollover that can be correlated from hanging-wall to footwall and draw it on the cross section with the geometry it had prior to displacement by the master fault. The restoration horizon need not be planar or horizontal.

2. Determine the shallow geometry of the structure. Locate the hanging-wall cutoff against the master fault, find the shape of the fault between the hanging-wall cutoff and the footwall cutoff and the shape of the sheet dip of the key bed within the rollover.

3. Calculate $e_{\parallel}$ from direct measurements of a representative bed length in the rollover compared to the length along the sheet dip between the same end points (equation 6) or from the domino geometry (equation 8).

4. Calculate α, the dip of the oblique simple-shear direction, using equation 4.

5. From the hanging-wall cutoff of the key bed against the master fault, draw a line of dip α that intersects the restoration horizon. This determines the horizontal displacement of the hanging wall, D.

6. Measure a length (l_1), in the α direction between the restoration horizon and the master fault, shift an amount D in the displacement direction and measure the same length downward in the α direction from the key bed to find a point on the fault. The

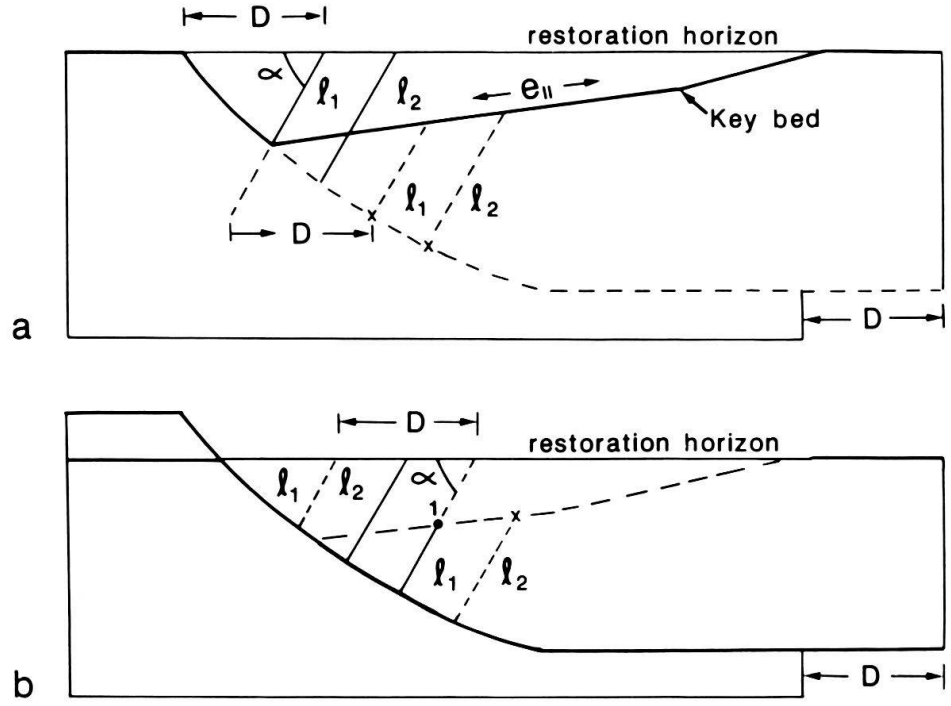

Fig. 6. Determination of fault shape and internal geometry of hanging wall by oblique simple-shear method (modified from VERRALL 1981). Solid lines are known, dashed lines computed. (a) Fault shape from geometry of a key bed. The strain parallel to bedding in this example is 10%. (b) Bed shape from fault geometry.

master fault is extended from its last known position to the new point. Repeat this process progressively from where the master fault is known toward the direction of fault displacement to define the complete fault geometry.

The more closely spaced the measurements, the better the definition of the fault shape. Errors in the determination of the fault shape between the hanging-wall cutoff and the footwall cutoff will be perpetuated along the reconstructed fault and may produce a wavy fault plane. A wavy fault plane can be smoothed or the shape of the updip master fault segment modified to obtain a satisfactory reconstruction.

After the fault plane is known, the sheet dip of any bed in the hanging-wall can be reconstructed following the method of VERRALL (1981), modified for oblique simple shear (Fig. 6b). One point on the rollover of the bed must be known, together with the direction of shear and the appropriate restoration horizon.

1. Define the restoration horizon geometry by correlating the key bed from footwall to hanging wall.

2. From the known point on the key bed (1, Fig. 6b), measure the length l_1 parallel to α. Move this length up the fault, maintaining the dip α, until it touches the restoration horizon. The horizontal distance D is the hanging-wall displacement of the key bed. In growth faults this value of D may be different from the value of D obtained from any other bed.

3. Measure a second length l_2, shift in the direction of displacement an amount D and measure up from the fault, along the direction α, to determine a new point (x) on the key bed. Repeat until the shape of the key bed is adequately defined.

Examples

The inversion technique is confirmed by comparison to the results of two experimental models, one sand and one clay, and is then applied to a seismic line from the Malawi rift where the result proves to be consistent with other estimates of the depth to detachment.

The sand model is from McClay & Ellis (1987a) for which the ramp portion of the master fault is a precut surface of wood. The uppermost sand bed and the master fault geometry are solid lines in Figure 7a. The bed shows localized thinning instead of discrete faults, consequently the extension in the rollover was determined by area restoration of the bed. The cross sectional area in the limb of the bed shown was measured and divided by its thickness in the graben, presumed to be the original thickness of the layer, to determine the original length. The final bed length in the limb is the length of the sheet dip. The layer-parallel extension is 53%, the sheet dip 24° and the calculated shear plane dip (eq. 4) is 57° antithetic. This is close to being opposite to the master fault dip of 59°. The constructed fault plane is the dashed line in Figure 7a. The match to the true fault plane is good, especially with regard to the depth to detachment. This example is also interesting because the published line drawing shows the zones of bed thinning as faults, an interpretation that results in a different value for the layer-parallel extension. From the interpretive line drawing of McClay & Ellis (1987a) the layer-parallel extension for the bed in Figure 7a is 29%, the dip of the shear plane 79° and the predicted depth to detachment is about twice the correct value. This demonstrates the sensitivity of the fault shape to the measurement of layer-parallel strain.

The clay model (Fig. 7b) is from Cloos (1968). The fault developed during the experiment, not as a precut. Small faults visible near the key bed are shown on the drawing. The sheet dip of the top horizon in the rollover is 14.5°, the layer-parallel extension 28% (calculated from the bed thinning: Groshong 1989, Table 1) and the dip of the shear plane (eq. 4) is 53° antithetic, exactly opposite to the average fault dip. The predicted fault is close to the true fault and nicely matches the depth to detachment.

The field example is seismic line 817 (Rosendahl 1987) from Lake Malawi, part of the Western Branch of the East African rift system. This profile was chosen because the rollover appears to return to the elevation of the restoration horizon obtained from the footwall. The seismic line has a vertical exaggeration of 3:1 but is reconstructed at 1:1 in Figure 7c. The limb of the half graben is broken by numerous parallel rotated fault blocks that are not shown in Figure 7c but have been used to calculate the layer-parallel strain using the domino model. From the true-scale profile, the sheet dip of the rollover is 2°, bedding in the domino blocks dips 3.4° making $\Theta^* = 1.4°$ and the domino-fault cutoff angle is 29.7°. The layer-parallel strain is found to be 4.5% (eq. 8) and the dip of the shear plane 39° antithetic (eq. 4). The near-surface dip of the master fault is 42°. The constructed depth to detachment is about 19 km (Fig. 7c). The depth to detachment is sensitive to the measured layer-parallel strain. If the strain were only 3% the shear angle would be 51° and the depth to detachment 23 km; layer-parallel strain of 9% gives a shear angle of 23° and a depth to detachment of 13 km. According to Bosworth (in Bosworth & Gibbs 1985), deep seismic reflection sections in the East African rift show detachments to be at 12–18 km depth. This is the depth range

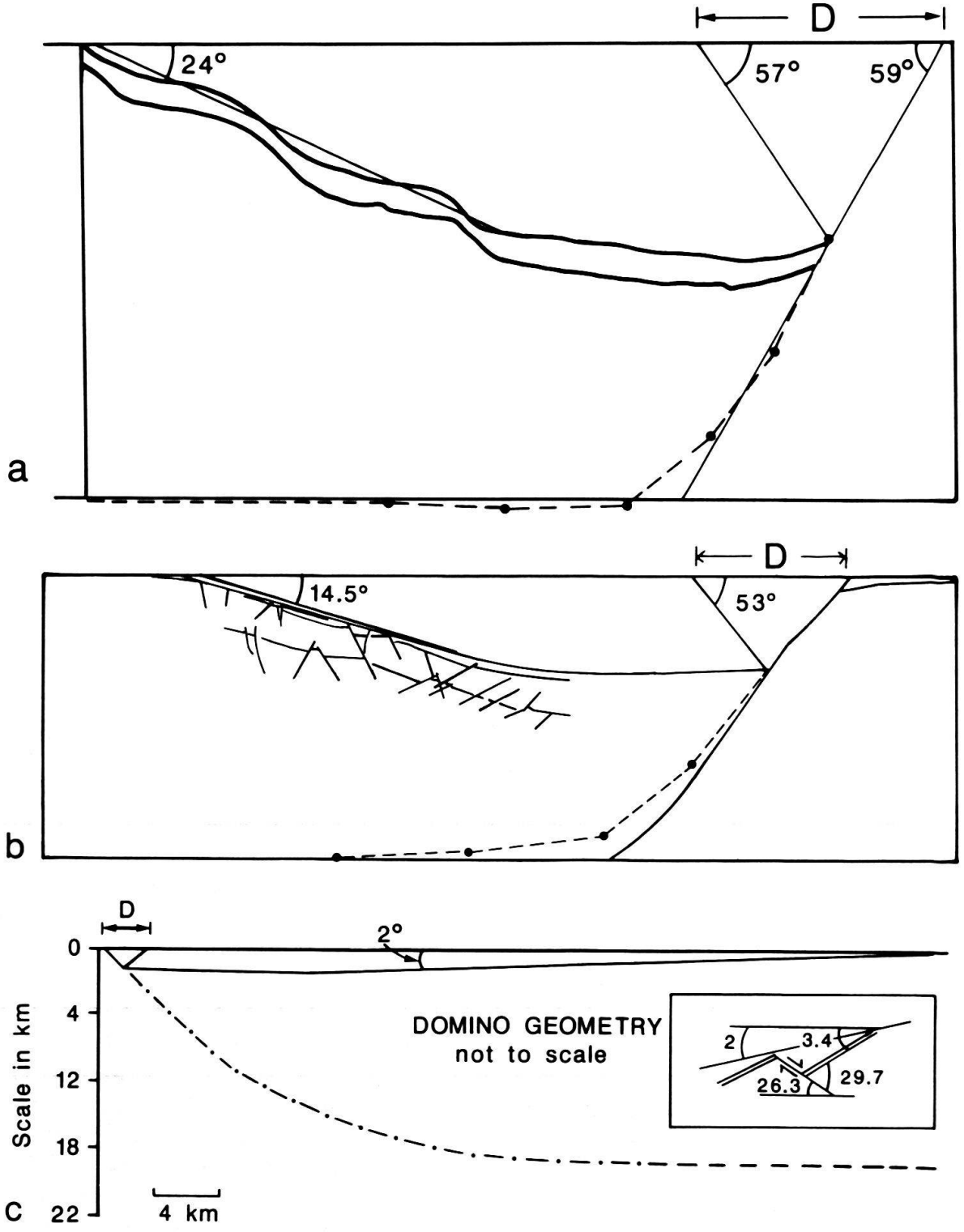

Fig. 7. Examples using the oblique simple-shear inversion for which the angle of shear is computed from the strain in the rollover. The computed shear angles are shown as lines antithetic to the upper fault segments. Solid lines are data, dashed lines are computed fault trajectories. (a) Sandbox model no. 93 from McClay & Ellis (1987a). The straight line dipping 24° on the limb indicates the orientation and length of the sheet-dip segment measured (b) Clay model S_5 from Cloos (1968). The sheet dip is 14.5°. (c) Depth-converted profile of top pre-rift sequence drawn from seismic line 817 across Lake Malawi, East African rift (Rosendahl 1987). Inset is average domino-block geometry in the dipping limb showing true angles (not to scale).

characteristic of the base of major extensional seismicity within cratons (Chen & Molnar 1983) which has been interpreted by numerous authors as the level of detachment. An earthquake at the south end of the Malawi rift occurred at a focal depth of 17 km (Shudofsky 1985). Shudofsky (1985) and Ebinger et al. (1987) state that earthquakes on the Western Branch of the African rift system are all less than 20 km deep, averaging 12–15 km, although Shudofsky (1985) reports a few in the 20–30 km depth range. The Krisp project (1987) obtained a reflection from an intracrustal discontinuity at 15 km in the Kenya rift. These data are broadly consistent with the depth to detachment inferred from the oblique simple shear model.

Discussion

Three assumptions about the geometry and internal deformation of the hanging wall have been made in order to use the hanging-wall geometry to find the fault shape.

1. The shape of the hanging wall of the independent half graben is directly related to the shape of the fault and to the amount of displacement.

2. The hanging-wall geometry to fault shape relationship is vertical or oblique simple shear.

3. The simple-shear direction is constant throughout the hanging-wall and throughout time. In the experimental models these assumptions must be correct to the first order for the model to have worked.

Three additional assumptions must be made in field examples in order to apply the method.

4. The geometry of a key bed in the rollover is accurately determined.

5. The layer-parallel strain in the key bed is measured correctly.

6. The restoration horizon, representing the shape and location of the key bed prior to displacement can be deduced.

Factors which may alter the assumed geometric relationships or affect the applicability of the inversion method include isostasy, compaction, ability to determine true dips from seismic data, and the ability to measure the strain in the key bed. Except for the problem of strain measurement, these factors can be treated by making suitable corrections to the observed data. Of these, the isostatic correction is probably the least certain. Regional isostatic changes should affect the hanging wall and footwall alike and so not cause a significant problem for the method, based, as it is, on the local geometry of the half graben. Mathematical models (Voorehoeve & Houseman 1988) as well as numerous field observations suggest that the most important local geometric change due to isostasy is footwall uplift which, however, appears to occur relatively independently of the hanging-wall geometry. The practical result of footwall uplift is to render uncertain the original elevation of the restoration horizon. Errors in the elevation of the restoration horizon produce errors of corresponding magnitude in the elevation of the lower detachment. Maximum footwall uplift occurs in the central regions of half grabens and dies out along-strike (Rosendahl 1987). The appropriate restoration horizon may, therefore, be found near the ends of the master fault.

The ultimate test of whether the various corrections have been made properly is the internal consistency of the complete solution. Different key beds should yield the same fault geometry and the predicted and known portions of the master fault should

match (WHITE et al. 1986; WHITE 1987; ROWAN & KLIGFIELD 1989). The method proposed here adds an additional constraint; the strain in the key bed should be consistent with the sheet dip of bedding in the rollover and with the angle of simple shear.

The fault geometry constructed for the two experimental models is listric, although both models have closer to a ramp-and-flat profile. The difference may be related to assumption 3 above, in that the angle of oblique simple shear may not have been perfectly constant throughout the experiment. The close agreement of the actual and predicted lower detachment horizons suggests that this is a second-order effect. The constructed fault profiles should be regarded as smoothed versions of the true profiles.

An important question related to the predicted master fault shape is whether all the layer-parallel strain in the rollover is visible as fault displacement at the scale of the cross section. In both sand and clay models, fault displacements accomplish only 40–80% of the total strain (KAUTZ & SCLATER 1988) which is why the average bed thickness is used here to measure the strain. In field examples of extension in the low-temperature environment, most of the strain is evidently by macroscopic faulting. To the writer's knowledge, large grain-scale strains have not been reported. Domino-block strain is independent of the size of the block as long as the sheet dip is maintained. Consequently, for the domino style of deformation, unobserved faults will not alter the computed strain. Unobserved small-scale full grabens within the rollover or strain within the domino blocks will cause the true strain to be greater than the measured value. As a result, the computed dip of the shear plane will be too large and the depth to detachment too great. For this reason the computed depth to detachment should be considered to be a maximum value. Where the master fault and key bed geometry are well known, the strain in the rollover can be computed from equation 2 or 3 and compared to the strain due to visible faults. A discrepancy between the amounts of strain could be due to the presence of unobserved faults. The method should, therefore, be of use in the prediction of unseen faults.

The strain vs. shear-plane-dip curves (Fig. 4) show that the strain in the rollover is very small for vertical simple shear. Many thin-skinned listric faults show little evidence of extension within the rollover (BALLY 1983; ROWAN & KLIGFIELD 1989) which is consistent with the success of vertical simple shear in matching the fault profiles (VERRALL 1981; ROWAN & KLIGFIELD 1989).

Zero layer-parallel strain solutions (Fig. 4) can be obtained with steeply dipping synthetic simple shear. Such a solution gives a constant bed-length cross section, just like a flexural-slip model. Constant bed length cannot be maintained throughout a simple-shear deformation history, however, unless the dip of the shear plane changes systematically through time. Thus oblique simple shear and constant bed length may both fit at a particular instant but the kinematic histories will differ.

The examples show that the best-fit oblique simple-shear direction in the hanging wall does not necessarily correspond to the deformation mechanism in the hanging wall. In the sand model, discrete faults did not develop although the zones of bed thinning, interpreted as faults, are antithetic to the master fault (MCCLAY & ELLIS 1987a). In the clay model, the strain in the upper levels of the rollover is by small conjugate faults (Fig. 7b), only one direction of which is close to the best-fit simple-shear direction. Deeper in the hanging wall the predominant direction of faulting is synthetic, not antithetic like the overall simple-shear direction. The strain in the hanging wall of the

example from Lake Malawi is by means of domino blocks for which the fault dip is synthetic, opposite to the required simple-shear direction. The beds within the rollover are required to strain parallel to bedding by an amount that can be computed from the geometries but the strain mechanism and fault geometries that accomplish the strain are independent of the geometry. The fact that the computed direction of oblique simple shear is nearly antithetic to the surface dip of the master faults may be a coincidence in the choice of examples and should be tested with other examples.

Conclusions

The layer-parallel strain associated with the oblique simple-shear model provides the additional information required to uniquely determine fault shape from the geometry of a single bed in the rollover of an independent half graben above a detachment. The method is fairly sensitive to sheet dip of bedding and the layer-parallel strain in the rollover, consequently the predicted fault geometry is closely constrained if these parameters are known well. Applied to experimental models, the method rounds off sharp bends in the fault profile but closely predicts the depth to detachment. In the East African rift example the predicted depth to detachment is consistent with that inferred from other data.

Acknowledgments

It is a pleasure to acknowledge the inspiration provided by Hans Laubscher. His research is replete with stimulating examples of the insight to be obtained by pursuing the quantitative consequences of an interpretation. This paper has benefitted from thoughtful reviews by W.A. Thomas, M.G. Rowan, T. Noack and H. Laubscher. The final form of equation 4 was suggested by Noack and Laubscher. R.D. Law suggested valuable references.

REFERENCES

Ashford, T. 1972: Geoseismic history and development of Rincon field, South Texas. Geophys. 37, 797–812.

Axen, G.J. 1988: The geometry of planar domino-style normal faults above a dipping basal detachment. J. Struct. Geol. 10, 405–411.

Bally, A.W. 1983: Seismic expression of structural styles, v. 2 – Tectonics of extensional provinces. Amer. Assoc. Petroleum Geol. Studies in Geol. Ser. 15.

Bally, A.W. & Snelson, S. 1980: Realms of subsidence. In: Facts and Principles of World Petroleum Occurrence (Ed. by Miall, A.D.). Canadian Soc. Pet. Geol. Mem. 6, 9–94.

Bally, A.W., Gordy, P.L. & Stewart, G.A. 1966: Structure, seismic data, and orogenic evolution of southern Canadian Rocky Mountains: Bull. Canadian Pet. Geol. 14, 337–381.

Beach, A. 1986: A deep seismic reflection profile across the northern North Sea: Nature 323, 53–55.

Bosworth, W. & Gibbs, A.D. 1985: Discussion on the structural evolution of extensional basin margins. J. Geol. Soc. London 142, 939–942.

Bucher, W.H. 1933: Deformation of the Earth's Crust: Princeton University Press, Princeton.

Chamberlin, R.T. 1910: The Appalachian folds of central Pennsylvania. J. Geol. 18, 228–251.

Chen, W.P. & Molnar, P. 1983: Focal depths of intracontinental and intraplate earthquakes and their implications for the thermal and mechanical properties of the lithosphere. J. Geophys. Res. 88, 4183–4214.

Cloos, E. 1968: Experimental analysis of Gulf Coast fracture patterns: Amer. Assoc. Petroleum Geol. Bull. 52, 420–444.

Crespi, J.M. 1988: Using balanced cross sections to understand Early Mesozoic extensional faulting. In: Studies of the Early Mesozoic basins of the eastern United States (Ed. by Froelich, A.J. & Robinson, G.R.). U.S. Geol. Surv. Bull. 1776, 220–229.

Dahlstrom, C.D.A. 1969: Balanced cross sections. Canadian J. Earth Sci. 6, 743–757.

Davison, I. 1986: Listric normal profiles: calculation using bed-length balance and fault displacement. J. Struct. Geol. 8, 209–210.

Doebl, F. & Teichmüller, R. 1979: Zur Geologie und heutigen Geothermik im mittleren Oberrhein-Graben. Fortschr. Geol. Rheinld. u. Westf. 27, 1–17.

Ebinger, C.J., Rosendahl, B.R. & Reynolds, D.J. 1987: Tectonic model of the Malawi rift, Africa. Tectonophysics 141, 215–235.

Ellis, P.G. & McClay, K.R. 1988: Listric extensional fault systems – results of analogue model experiments. Basin Res. 1, 55–70.

Eyidogan, H. & Jackson, J. 1985: A seismological study of normal faulting in the Demirci, Alasehir, and Gediz earthquakes of 1969–70 in western Turkey; implications for the nature and geometry of deformation in the continental crust. Geophys. J. Royal Astr. Soc. 81, 569–607.

Geiser, J., Geiser, P.A., Kligfield, R., Ratliff, R. & Rowan, M. 1988: New applications of computer-based section construction: strain analysis, local balancing and subsurface fault prediction. Mountain Geol. 25, 47–59.

Gibbs, A.D. 1983: Balanced cross-section construction from seismic sections in areas of extensional tectonics. J. Struct. Geol. 5, 153–160.

— 1984: Structural evolution of extensional basin margins. J. Geol. Soc. London 141, 609–620.

Gibson, J.R., Walsh, J.J. & Watterson, J. 1989: Modelling of bed contours and cross-sections adjacent to planar normal faults. J. Struct. Geol. 11, 317–328.

Groshong, R.H. Jr. 1989: Half-graben structures: Balanced models of extensional fault-bend folds. Geol. Soc. Amer. Bull. 101, 96–105.

Hamblin, W.K. 1965: Origin of "reverse drag" on the downthrown side of normal faults. Geol. Soc. America Bull. 76, 1145–1164.

Hansen, W.R. 1965: Effects of the earthquake of March 27, 1964, at Anchorage, Alaska. U.S. Geol. Surv. Prof. Pap. 542-A.

Kautz, S.A. & Sclater, J.G. 1988: Internal block deformation in clay models of extension by block faulting. Tectonics 7, 823–832.

Kligfield, R., Crespi, J., Naruk, S. & Davis, G.H. 1984: Displacement and strain patterns of extensional orogens. Tectonics 3, 577–609.

Krisp 1987: Structure of the Kenya rift from seismic refraction. Nature 325, 239–242.

Laubscher, H.P. 1962: Die Zweiphasenhypothese der Jurafaltung. Eclogae geol. Helv. 55, 1–22.

— 1965: Ein kinematisches Modell der Jurafaltung. Eclogae geol. Helv. 58, 231–318.

— 1982: Die Südostecke des Rheingrabens – ein kinematisches und dynamisches Problem. Eclogae geol. Helv. 75, 101–116.

Le Pichon, X. & Sibuet, J.-C. 1981: Passive margins: A model of formation. J. Geophys. Res. 86, 3708–3720.

Mandl, G. 1987: Tectonic deformation by rotating parallel faults: the "bookshelf" mechanism. Tectonophysics 141, 277–316.

McClay, K.R. 1987: The mapping of geological structures: Halsted Press, John Wiley & Sons, New York.

McClay, K.R. & Ellis, P.G. 1987a: Analogue models of extensional fault geometries. In: Continental extensional tectonics (Ed. by Coward, M.P., Dewey, J.F. & Hancock, P.L.). Geol. Soc. Special Pub. No. 28. Blackwell Scientific Publications, Oxford, 109–125.

— 1987b: Geometries of extensional fault systems developed in model experiments. Geol. 15, 341–344.

Miller, E.L., Gans, P.B. & Garing, J. 1983: The Snake Range decollement: an exhumed mid-Tertiary ductile-brittle transition. Tectonics 2, 239–263.

Morton, W.H., & Black, R. 1975: Crustal attenuation in Afar. In: Afar Depression of Ethiopia, 1 (Ed. by Pilger, A. & Rosler, A.). Schweizerbart'sche Verlagsbuchhandlung, Stuttgart, 55–65.

Rosendahl, B.R. 1987: Architecture of continental rifts with special reference to East Africa. Ann. Rev. Earth and Planet. Sci. 15, 445–503.

Rowan, M.G. & Kligfield, R. 1989: Cross section restoration and balancing as aid to seismic interpretation in extensional terranes: Amer. Assoc. Petroleum Geol. Bull. 73, 955–966.

Sclater, J.G. & Célérier, B. 1988: Errors in extension measurements from planar faults observed on seismic reflection lines. Basin Res. 1, 217–221.

Scott, D.L. & Rosendahl, B.R. 1989: North Viking Graben: An East African perspective. Amer. Assoc. Petroleum Geol. Bull. 73, 155–165.

Shudofsky, G.N. 1985: Source mechanisms and focal depths of East African earthquakes using Raleigh wave dispersion and body-wave modelling. Geophys. J. Royal Astr. Soc. 83, 563–614.

Stewart, J.H. 1971: Basin and Range structure: A system of horsts and grabens produced by deep-seated extension. Geol. Soc. Amer. Bull. 82, 1019–1044.

Suppe, J. 1983: Geometry and kinematics of fault-bend folding. Amer. J. Sci. 283, 684–721.

Thompson, G.A. 1960: Problem of late Cenozoic structure of the Basin Ranges. Proc. 21st Internat. Geol. Cong. Copenhagen 18, 62–68.

Vendeville, B., Cobbold, P.R., Davy, P., Brun, I.P. & Choukroune, P. 1987: Physical models of extensional tectonics at various scales. In: Continental extensional tectonics (Ed. by Coward, M.P., Dewey, J.F. & Hancock, P.L.). Geol. Soc. Special Publication No. 28. Blackwell Scientific Publications, Oxford, 95–107.

Verrall, P. 1981: Structural interpretation with applications to North Sea problems. Course notes. Joint Association Petroleum Exploration Courses (JAPEC), London.

Voorhoeve, H. & Houseman, G. 1988: The thermal evolution of lithosphere extending on a low-angle detachment zone. Basin Res. 1, 1–9.

Wernicke, B. & Burchfiel, B.C. 1982: Modes of extensional tectonics. J. Struct. Geol. 4, 105–115.

Wheeler, J. 1987: Variable-heave models of deformation above listric normal faults: the importance of area conservation. J. Struct. Geol. 9, 1047–1049.

White, N. 1987: Constraints on the measurement of extension in the brittle upper crust. Norsk Geol. Tidssk. 67, 269–279.

White, N.J., Jackson, J.A. & McKenzie, D.P. 1986: The relationship between the geometry of normal faults and that of the sedimentary layers in their hanging-walls. J. Struct. Geol. 8, 897–909.

Williams, G. & Vann, I. 1987: The geometry of listric normal faults and deformation in their hangingwalls. J. Struct. Geol. 9, 789–795.

Woodward, N.B., Boyer, S.E. & Suppe, J. 1989: Balanced geological cross-sections: An essential technique in geological research and exploration. Amer. Geophys. Union. Short Course in Geology, 6.

Manuscript received 18 January 1990
Revision accepted 18 July 1990